Evaluation of Solar Panel Bandwidth for RGB Channels in Visible Light Communication

R. A. Martínez-Ciro, F. E. López-Giraldo, J. M. Luna-Rivera, J. D. Rojas-Usuga, and J. D. Navarro-Restrepo

***Abstract*—Visible light communication (VLC) is an emerging technology that uses white light-emitting diodes (LEDs) to transmit information and provide illumination simultaneously. Recently, solar panels have been proposed as optical detectors at the receiver to retrieve data from light signals. However, very few studies have addressed the behavior of the solar panel bandwidth at different wavelengths. In this paper, we propose the design of a low-complexity VLC system with a red-green-blue (RGB) LED transmitter and a solar panel receiver whose bandwidth is modified using a parallel load resistor. We define a set of experiments to validate the performance of the VLC system using an RGB LED source and a solar panel as the optical receiver. The VLC system's performance is evaluated across various baud rates (4800, 9600, 19200, 38400, 57600, and 115200 bits/s) at a free space transmission distance of less than 105 cm. Our measurements indicate that the solar panel's highest bandwidth is achieved with the red channel, yielding a maximum data rate of 57600 bits/s at a bit error rate (BER) of 5×10^{-3}. These results are analyzed and discussed to highlight the benefits and limitations of using solar panels for VLC purposes.**

Link to graphical and video abstracts, and to code: https://latamt.ieeer9.org/index.php/transactions/article/view/8516

***Index Terms*—Visible light communication, Optical wireless communication, Solar panel, RGB LED**

I. Introduction

Wireless communication systems have significantly contributed to the rapid economic growth and development of modern society [1, 2]. However, the continuous demand for higher data rates by mobile phones and other wireless devices has led to spectrum shortages [3]. As a result, Visible Light Communication (VLC) has garnered considerable interest as an alternative technology to address spectrum scarcity [4]. The first VLC standard, known as IEEE 802.15.7, has been proposed for the upcoming generation of optical wireless communication [5]. VLC uses the visible spectrum to provide wireless communications and illumination at the same time [6–8]. This technology operates in the 400 to 700 nm range, is highly directional, and offers a high level of physical link security [6, 7]. The advantages of VLC systems encompass a license-free spectrum, no radio frequency interference, a directional communication link, low-cost connectivity, and the potential for high data rates [7].

VLC systems are composed of a light-emitting diode (LED) as a transmitter and an optical receiver which can be implemented using a photodiode (PD) [6, 9], RGB sensor [10], a light-to-frequency (LTF) converter [11], a camera [12, 13], or a solar panel [14]. The transmitter can use white LEDs or RGB LEDs due to their low cost, high-performance energy, and useful bandwidth, enabling the development of high-speed data transmission VLC systems [15]. On the receiver side, positive-intrinsic negative (PIN) PD is the most common photodetector used in VLC systems. Additionally, the use of PDs with RGB optical filters [16, 17], employing color-shift keying (CSK) modulation can improve further the transmission rate of VLC systems [18, 19]. Since a solar panel can directly convert photon power into electrical current without requiring an external power source, there is a potential opportunity for this type of passive device to be also used as a VLC receiver. The main advantage of using a solar panel as a VLC receiver (Rx) is the simplicity of the receptor design, which removes the need for a transimpedance amplifier [18–20]. Several studies have examined the design of solar panel-based receivers for simultaneous optical wireless communication (OWC) and energy harvesting [14]. In particular, some encouraging results have been reported when a parallel load resistance circuit is employed at the solar panel-based receiver [14]. These results have proved the potential of VLC for future low power applications in optical wireless communication. Moreover, the spectral efficiency of orthogonal frequency division multiplexing (OFDM) was also adopted to enhance the data rate of a VLC system based on the solar-panel receiver. However, OFDM requires high-speed digital signal processing (DSP) for modulation/demodulation processes. Therefore, an important issue in the literature has been directed toward the development of a low complexity VLC system with receivers based on solar panels [21–24]. Moreover, understanding the performance of solar panels using different light color channels can be particularly advantageous for cost-sensitive Internet-of-Things (IoT) networks. By identifying the most efficient wavelengths for power conversion—explored in the context of photo-luminescence modulation for optical frequency identification devices [21]—IoT devices can be optimized to use fewer and smaller panels, significantly reducing hardware costs. This is especially crucial in IoT applications where device proliferation is high and operational costs need to be minimized, such as in sensor networks for smart agriculture, energy management systems in smart homes, and wearable

R. A. Martínez-Ciro, F. E. López-Giraldo, J. D. Rojas-Usuga and J. D. Navarro-Restrepo are with the Instituto Tecnológico Metropolitano of Colombia, Medellin, Colombia (e-mails: rogermartinez@itm.edu.co, franciscolopez@itm.edu.co, juanrojas166633@correo.itm.edu.co and juannavarro139070@correo.itm.edu.co).

J. M. Luna-Rivera is with Autonomous University of San Luis Potosí, México (e-mail: mlr@uaslp.mex).

health monitoring devices. The precise tuning to the most effective wavelengths means not only lower initial setup costs but also improved energy efficiency, leading to long-term savings and sustainability benefits. Thus, our investigation into the wavelength-dependent performance of solar panels provides key insights for the economical and ecological design of future IoT infrastructure.

This paper investigates the utility of a commercially available solar panel as an optical receiver within a VLC system, employing RGB LEDs as the light source. Unlike previous studies, such as reference [14] which focuses on using solar panels for both data transmission and energy harvesting in optical wireless communications, our primary goal is to characterize the solar panel's performance by analyzing its bandwidth and spectral response to varying wavelengths emitted by RGB LEDs. These LEDs offer the advantage of parallel communication channels with minimal interference, a feature not extensively explored in references [21–24], which cover topics ranging from luminescent emissions to pre-distortion techniques for performance enhancement. As the RGB LEDs' optical power incidents on the solar panel surface, it enables us to evaluate the spectral response of the optical signals received by the solar panel [25]. We demonstrate that digital modulation, facilitated by an affordable microcontroller, simplifies both modulation and demodulation processes. Our approach diverges from the referenced studies by emphasizing the relationship between different light wavelengths and the VLC system's performance, especially regarding data rates and bit error rates, which is a novel aspect not covered in these references.

The versatility of this approach is underscored by its compatibility with wavelength division multiplexing, broadening potential applications to include access control, Internet of Things (IoT) devices, indoor positioning, and audio streaming. We present the evaluation of the solar panel bandwidth using an RGB LED optical source, experimental demonstrations of a VLC system based on the solar panel receiver using the OOK modulation scheme, and the design of experiments to evaluate the solar panel as a VLC receiver. These include determining the optical-to-electrical response of the solar panel with multicolor LED sources, measuring the frequency and bandwidth responses at different wavelengths, and validating performance in a VLC system with RGB LED channels.

Our findings reveal that the solar panel bandwidth varies with LED wavelengths, achieving peak data rates with the red channel. We offer an analysis of various baud rates over a free-space transmission distance of up to 105 cm, using universal asynchronous receiver/transmitter (UART) for serial communication. The results not only indicate the optimal pairing of RGB LED channels with generic solar panels for OWC applications but also highlight the potential for low-cost, low-bit-rate VLC applications. Future work will focus on integrating energy harvesting with communication services, enhancing RGB channel performance, refining analog equalization techniques, and investigating wavelength-division multiplexing strategies to maximize VLC system capacity.

The rest of this paper is organized as follows. Section 2 provides a general overview of the VLC system and solar panel-based receiver model. Section 3 describes the methodology implemented in this study: calculation of the OE response of the commercial solar panel used for RGB LED optical power source; measurement of the frequency response of the solar panel receiver, and experimental validation of the VLC system with a solar panel-based receiver. The overall results and discussion are given in Section 4. Finally, the conclusion will be presented in Section 5.

II. Visible Light Communication System with a Solar Panel-Based Receiver Model

A. VLC System Model

Fig. 1 presents a block diagram of a standard white LED-based VLC system. At the transmitter, the information data signal passes through the modulator which is responsible for the bias electrical current variation of the LED, $i_t(t)$. The white LED includes a blue LED with a bandwidth (BW) of 12 MHz covered with a phosphor layer that degrades its performance at 3 MHz [24–26]. The modulated light, transmitted through a Line-of-Sight (LOS) optical channel, propagates directly to the receiver without obstructions, ensuring reliable data transmission. When the photodiode detects incident optical power, $P_t(t)$, on its photosensitive surface, it generates a photocurrent, $i_r(t)$, proportional to the sensor's responsiveness $R(\lambda)$ as a function of wavelength. This current, which is corrupted by additive white Gaussian noise, $n(t)$, reflects the direct signal transmission afforded by the LOS channel, a setup commonly adopted in laboratory experiments for its simplicity and efficacy [26]. Such a relation is calculated as:

$$i_r(t) = P_t(t)R(\lambda) + n(t). \tag{1}$$

For a more general optical wireless communication system, the current $i_r(t)$ at the output of the photodetector can also be expressed as follows:

$$i_r(t) = R(\lambda)\left[i_t(t) \bigotimes h_{eo}(t) \bigotimes h(t)\right] + n(t), \tag{2}$$

where $h(t)$ is the optical channel impulse response; $h_{eo}(t)$ denotes the impulse response of the LED circuit, $i_t(t)$ is the bias current of LED and $\bigotimes$ the convolution operator.

B. Solar Panel Receiver Model for Optical Wireless Communication

Solar panels are designed to use solar radiation to generate electricity. Although some improvements in manufacturing costs have helped make solar panels affordable, their efficiency

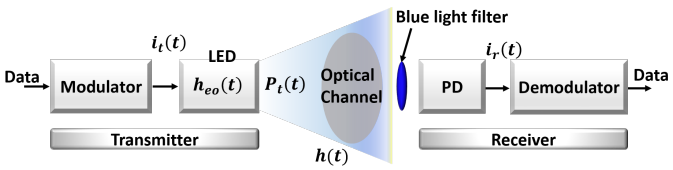

Fig. 1. Visible light communication system scheme based white LED and PD.

is still considered low [27]. In recent years, solar panels have attracted significant interest in the literature for VLC applications [22]. Therefore, the development of an efficient and low-cost solar panel receiver for VLC has been an active research topic. In [14], Wang et al. proposed the design of a solar panel-based OWC receiver capable of simultaneous communication and energy harvesting. Under this approach, an equivalent model of the solar panel for communication purposes is shown in Fig. 2. It includes the light-generated current in the panel, that comprises a direct current (DC) component, i_{DC}, of the solar panel plus the alternating current (AC) component, $i_{PH}(w)$, of the photocurrent collected by the solar cells for communication purposes. The shunt resistor R_{SH} and capacitor C model the leakage current and internal capacitive effects in the solar cells. Since a solar cell can be modeled as a diode in parallel with a current source, the parameter r defines the equivalent resistor model for the diode. The L series inductor models the inductance of any wire connection to the solar panel. Finally, the parasitic resistor R_S represents the voltage drop across the cell interconnections. We remark that this communication system conveys information through the output voltage $v(w)$ of the load resistor R_L where the information is encoded on the AC component of $v(w)$.

Consequently, and following the same analysis as in [14], the frequency response of the solar panel circuit can be calculated as:

$$\left|\frac{v(w)}{i_{PH}(w))}\right|^2 = \left|\frac{\frac{R_L}{R_S+jwL+R_L}}{\frac{1}{r}+\frac{1}{\frac{1}{jwC}}+\frac{1}{R_{SH}}+\frac{1}{R_S+jwL+R_L}}\right|^2, \quad (3)$$

where w is the angular frequency and $j=\sqrt{-1}$.

III. Experimental Design

The experiments were conducted in the laboratory under controlled light conditions to reduce the DC component induced in the solar panel by external light sources, and because the AC component has a small variation compared to the magnitude of the DC [14]. In our experiment, the AC component is an important parameter to evaluate the solar panel-based receiver for a visible light communication system. The implementation consists of three different setups. Firstly, we describe the experimental setup for measuring the optical-to-electrical (OE) response of the solar panel at different wavelengths. We considered exploring a commercial and low-cost PV panel, such as polycrystalline. It should be noted that temperature can also affect the performance of the solar panel [28], but was not considered in this initial study. Experiments were conducted in the laboratory at a controlled temperature of $20°C$. Then, a second experiment is designed to evaluate the solar-panel bandwidth characteristics using an RGB LED as a transmitter. Finally, experimental validation of a complete VLC system with solar panel receiver is presented.

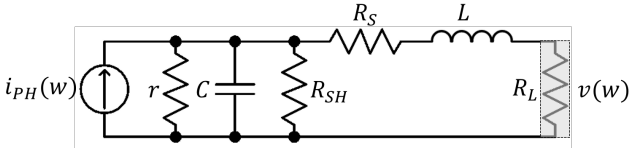

Fig. 2. Solar cell equivalent circuit model for OWC [14].

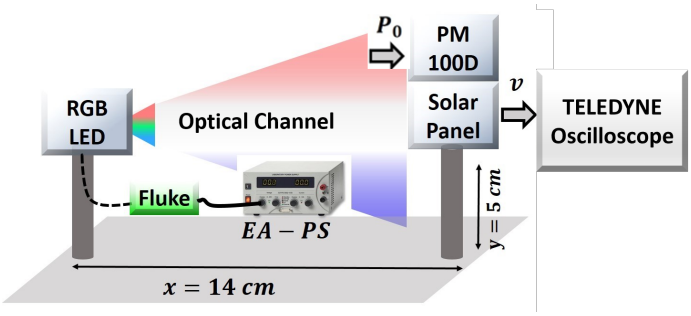

Fig. 3. Experimental setup to determine the optical-to-electrical response of the solar panel.

A. OE Response of the Solar Panel Receiver

Fig. 3 illustrates the laboratory experimental setup designed to measure the optical-to-electrical conversion capabilities of the solar panel with a physical area of 66 cm^2 using a 5050-RGB LED source. The bias current for the RGB LED, which is critical for controlling the intensity of the emitted light, was supplied by an EA-PS 3016-20B power source. Additionally, a Fluke 117 multimeter was employed to accurately measure this current, ensuring precise control over the LED's operation. The RGB LED was strategically positioned at a height of 5 cm from the solar panel receiver, optimizing the balance between light intensity and distribution for effective VLC system functioning.

The optical power emitted from each color channel was quantified using an S120C optical sensor connected to a Thorlabs PM100D optical power and energy meter console. The solar panel, along with the Thorlabs PM100D, was placed 14 cm away from the RGB LED source, maintaining a Line-of-Sight (LOS) optical channel. This configuration ensures unobstructed light propagation and reliable power measurement. The optical power measured at the solar panel's surface was consistently $P_0 = 10.6\ \mu W$, a parameter that remained constant throughout our experiments for uniform testing conditions. This optical power, P_0, was directed to the TELEDYNE oscilloscope for detailed analysis.Consequently, the solar panel generated a voltage output directly proportional to the incident optical power for each color channel, showcasing the direct and reliable signal transmission characteristic of the LOS optical setup used in our experiments.

B. Bandwidth Response of the Solar Panel for the VLC System

The experiment depicted in Fig. 4 was conducted to evaluate and determine the frequency response of the solar panel when used as a VLC receiver within a Line-of-Sight (LOS) optical channel configuration. For this proof-of-concept demonstration, we utilized a 5050-RGB LED with forwarding voltages of $2V$, $3V$, and $3V$ for the red, green, and blue channels, respectively. We harnessed the RIGOL DG162 arbitrary waveform generator (AWG) to supply the precise AC waveform

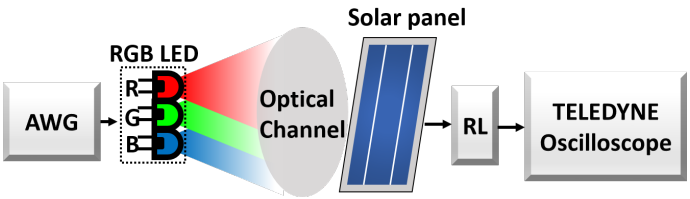

Fig. 4. Experimental setup to determine the bandwidth of a solar panel with a physical area of 66 cm^2.

that drove the RGB LED. This AWG, acting as a digital-to-analog converter (DAC), possesses an analog bandwidth of 160 MHz and a sampling rate of 500 MSa/s, facilitating the implementation of a frequency sweep for each RGB LED channel individually. The VLC RGB light signals emitted by the LED were then allowed to propagate across varying free space distances before being detected by the solar panel, characterized by an operational voltage and current of $V_{op}/I_{op} = 6V/167\ mA$ and an area of 66 cm^2.

Subsequently, the solar panel's output was fed into a Teledyne WAVEACE 2032 real-time oscilloscope (RTO), functioning as an analog-to-digital converter (ADC) with an analog bandwidth of 300 MHz and a sampling rate of 2 GSa/s. The RTO captured the AC waveform of the light signal received, which was subsequently analyzed on a personal computer using Matlab. Through this process, the solar panel's ability to convert the energy of multi-colored light into a proportional voltage was assessed. We determined the bandwidth of the solar panel by measuring the voltage at the $-3\ dB$ point, conducting this measurement both without a load resistor and with varying load resistors of 1 $k\Omega$, 5 $k\Omega$, and 10 $k\Omega$, each having a tolerance of 1%.

C. Performance Validation of the Solar Panel Receiver for Visible Light Communication System

Fig. 5 illustrates the experimental setup of the VLC system utilizing a solar panel as the receiver. In this configuration, two personal computers (PC1 and PC2) served as a pseudo-random byte generator and for data recovery, respectively, with both interfacing through Matlab. The data from PC1 were conveyed via a serial communication interface adhering to the RS232 standard to the microcontroller. We employed commercially available microcontrollers (ATmega328P, MCU1 and MCU2) equipped with a 16 MHz quartz crystal and a Universal Asynchronous Receiver/Transmitter (UART) for this task. The output data from MCU1 were transmitted to a Linear Variable Current Driver (LVCD), modulating the intensity of light from the RGB LED, which then emitted signals through a free-space optical channel. This channel ensured unobstructed transmission of the lightwave signal to the solar panel, which converted it into an electrical signal.

We methodically assessed the system's performance using red, green, and blue LEDs. The solar panel, specified in [14], functioned both as a VLC receiver and for energy harvesting. Following detection, a pulse reconstruction block within the system regenerated the original electrical bitstream, which MCU2 then relayed back to PC2 via serial communication. Finally, PC2 decoded the received signal, and the data were analyzed using Matlab, allowing for a comprehensive evaluation of the system's performance across the RGB spectrum.

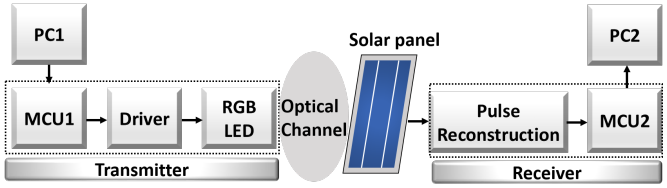

Fig. 5. Experimental setup of the VLC using a solar panel as the receiver. MCU: microcontroller unit, PC: Personal Computer.

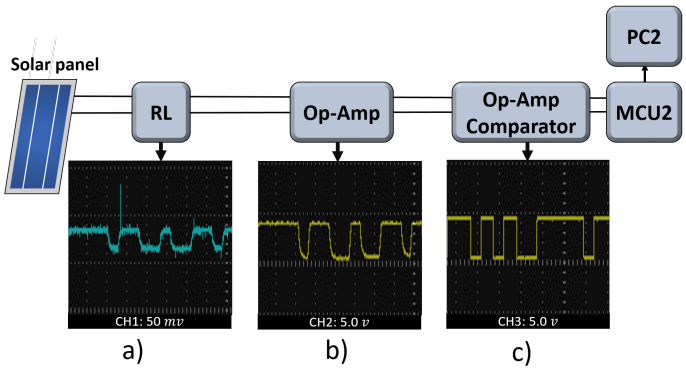

Fig. 6. Proposed solar panel-based receiver for visible light communication. (a) Waveform measurement with a digital oscilloscope on load resistor R_L (1 $k\Omega$) connected in parallel to the solar panel. (b) Electrical signal conditioned with an operational amplifier. (c) Original electrical bit stream regenerated by an Op-Amp comparator.

We used Matlab to design the pseudo-random byte generator (data=1MB) in PC1. Then, the constructed data were sent to MCU1 via UART communication using different baud rates. We conducted the experiments with different baud rates in a bit-serial format, specifically 4800, 9600, 19200, 38400, 57600, and 115200 $bits/s$ under 105 cm free space transmission distance. The visible light communication link has been tested for each baud rate. First, we set a baud rate of 4800 $bits/s$ to the RGB LED via the LVCD driver module and MCU1, which were then received by the solar panel. The limited bandwidth response of the solar panel in our experiments led to a degradation of the received electrical signal. To mitigate this, the pulse reconstruction process for the electrical bit stream from the solar panel receiver consists of several critical steps. As depicted in Fig. 6a-c, the stages are as follows: (a) Waveform Measurement, where we initially capture the waveform of the light-modulated signal using a digital oscilloscope across a load resistorR_L (1 $k\Omega$) connected in parallel to the solar panel. (b) Signal Conditioning involves using an operational amplifier (Op-Amp) to amplify and stabilize the electrical signal from the solar panel. The final stage, (c) Bit Stream Regeneration, employs an Op-Amp comparator to regenerate the original electrical bit stream, converting the conditioned analog signal back into a digital format, as seen in the recovered modulated signal.

Fig. 6a shows the received distorted signal due to the effects of charging and discharging cycles of the solar panel and

the parallel load resistance (R_L). The effect of the parallel resistor R_L (1 $k\Omega$) with the solar panel has an impact on BW of the system (in this case the solar panel) [14]. The BW decreases with high R_L values ($>$ $k\Omega$) and increases with low R_L values. However, for an adequate BW of the solar panel with $R_L = 1k\Omega$, the waveform of the received signal is distorted due to the slow charging and discharging effect of the solar panel (see Fig. 6a). Besides, we can also observe the DC baseline wandering issue. To reduce the DC baseline, we used a capacitor (1 μF) with input to an operational amplifier. It was necessary to amplify the voltage of the electrical signal with an operational amplifier (Op-Amp) (LM358P) (see Fig. 6b). The Op-amp was configured with a gain of 40 dBV and a standard 5V power supply. On the other hand, the Op-Amp comparator compared the analog voltage level of the received modulated signal with the reference analog voltage level and produced an output signal based on this comparison (the value of the output voltage depends on the Op-Amp power supply voltage). Fig. 6c illustrates the implementation of the Op-Amp voltage comparator (with a reference voltage of $2.5V$) to regenerate the original electrical signal with an amplitude between 5 (high) and 0 (low) volts. The voltage level of the output is high when the reference voltage is greater than the voltage of the bit-stream, and the voltage level of the output is low when the reference voltage is below the voltage of the bit stream. Finally, the reconstructed electrical signal was sent to PC2 via a MCU2, and the bit error rate (BER) of the received signal was analyzed using Matlab.

IV. Results

This section provides information about the performance of the solar panel-based receiver for the visible light communication system. Such information is presented in terms of the solar panels OE and frequency response to each RGB channel. During the experiments, there were no external sources of illumination that could be received by the solar panel receiver.

Table I shows the solar panels OE response which is compared to the optical power generated by the RGB LED channels. The bias current through the RGB LED was adjusted such that the incident optical power (P_o) on the solar panel was approximately 10.6 μW. The red-light of the LED was the component that consumed the most forward current (IF) and forward voltage (FV) for the same level P_o. However, it generated the highest solar panel voltage (SPV). It can be observed that the wavelength of the red light increased the solar panel's OE response. This experiment was carried out considering an open circuit solar panel ($R_L \to \infty\Omega$).

TABLE I
Solar Panels OE Response to RGB LED Optical Power

Variable	Red LED	Green LED	Blue LED	Symbol	Unit
Forward Voltage	10.3	7	7	FV	V
Forward Current	31.63	11.2	9.62	IF	mA
Optical Power	10.57	10.59	10.6	P_o	μW
Solar Panel Voltage	2.213	2.189	2.114	SPV	V

Table II lists the maximum-solar panel voltage ($maxSPV$) for different R_L values. The optical input power of the solar panel produces voltages of approximately equal magnitude. Therefore, in equal conditions, the responsivity between the RGB LED and the solar panel should be similar. Hence, we remark that the different responsivity values of each RGB channel show the viability of implementing multi-color modulation schemes, such as CSK [18, 19], in a VLC system with a solar-panel receiver.

TABLE II
Maximum Solar Panel Voltages with RGB LED Source and Different R_L Values

Variable	Red LED	Green LED	Blue LED	Symbol	Unit
No R_L	540	1020	880	$maxSPV$	mV
R_L $1k\Omega$	24	57.6	44	$maxSPV$	mV
R_L $5k\Omega$	104	292	226	$maxSPV$	mV
R_L $10k\Omega$	204	528	428	$maxSPV$	mV

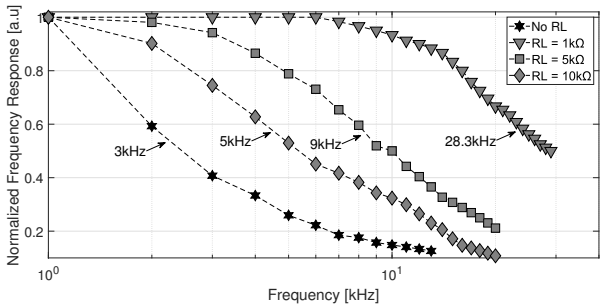

(a) Red LED channel

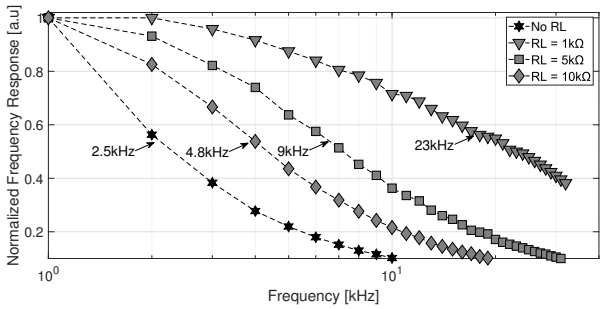

(b) Green LED channel

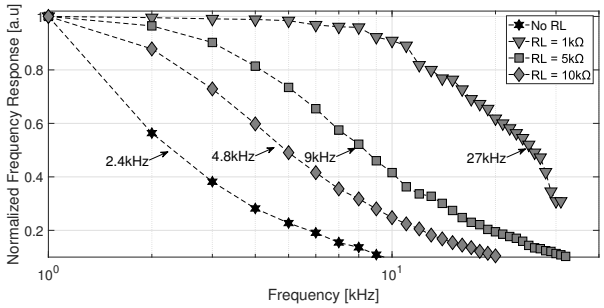

(c) Blue LED channel

Fig. 7. Frequency response of solar panel for different RGB LED channels and for various values of R_L, in the range from 1 $k\Omega$ to 10 $k\Omega$.

The frequency response of the solar panel configuration, presented in Fig. 4, was measured for different values of R_L, for each RGB LED channel. We have added a capacitor of

$1\ \mu F$ at the input of the oscilloscope TELEDYNE to block the DC component of the signal. Fig. 7 shows the solar panel frequency response versus the optical power of the RGB LED channels for different values on the load resistance R_L. Note that the points marked in Fig. 7 are for reference, since the bandwidth was estimated at -3 dB for each frequency response of the RGB channels [10]. The frequency response is normalized and built with the maximum voltage generated by the solar panel per frequency. The bandwidth response of the solar panel depends on the load resistance R_L and the wavelength of the light source. This measurement was taken for various values of R_L from $1\ k\Omega$ to $10\ k\Omega$. We can notice significant effects on the communication performance of the solar panel for each RGB LED. From the results in Fig. 7, it is concluded that as the resistor R_L ($k\Omega$) increases, the solar panel reduces its frequency response. Observe that the response is better, in terms of solar panel bandwidth, for the Red LED channel with $28.3\ kHz$ (Fig. 7a) than the Blue LED channel (Fig. 7b) and the Green LED channel (Fig. 7c) with $27\ kHz$ and $23\ kHz$ respectively.

We remark that the values for R_L are different from those used in [14] because the solar panel voltage was higher (see Table II). Additionally, the solar panel output voltage is proportional to the sensitive area and the efficiency of the cells at some illumination levels [14]. Therefore, the low resistance used in [14] is justified because of the larger area of the solar panel ($432\ cm^2$) as compared to the solar panel area ($66\ cm^2$) in this work. Hence, we highlight that the use of a larger solar panel would affect communication performance. Moreover, another disadvantage of such solar panels is that large physical dimensions can also affect installations, therefore, it is not convenient in those applications with hardware constraints.

Fig. 8 depicts the voltage response of the solar panel when subjected to maximum bandwidth conditions and the waveforms elicited by each light source. Notably, the red LED, when paired with a $1\ k\Omega$ load resistor, exhibits a higher bandwidth (as shown in Fig. 7a), although it results in a lower maximum solar panel voltage (maxSPV), as detailed in Table II. This leads to a reduced SNR, which is evident from the waveform's distortion attributed to the solar panel's slower charge and discharge rates (refer to Fig. 8a). The higher noise observed in the red channel's graph can be attributed to the solar panel's lower electro-optical response at this wavelength, necessitating the use of a $1\ k\Omega$ load resistor to improve the frequency response despite yielding a lower voltage signal. Consequently, more precise tuning of the window comparator was required to accurately reconstruct the electrical pulses for the digital communication process. For the green and blue LED channels, as illustrated in Fig. 8b and Fig. 8c, the solar panel's bandwidth decreases, yet the voltage signals for these channels are less distorted. This lower distortion is beneficial for the communication system's performance since voltage distortion can adversely affect the accurate estimation of the received information signal necessary for the demodulation process.

The other relevant solar panel application in OWC is in energy harvesting mode. In this case and according to Table II, we recommend using the green LED channel and not using the R_L resistor. However, it is interesting to note that in terms of solar panel bandwidth, it was lower for the green LED channel compared to the other channels.

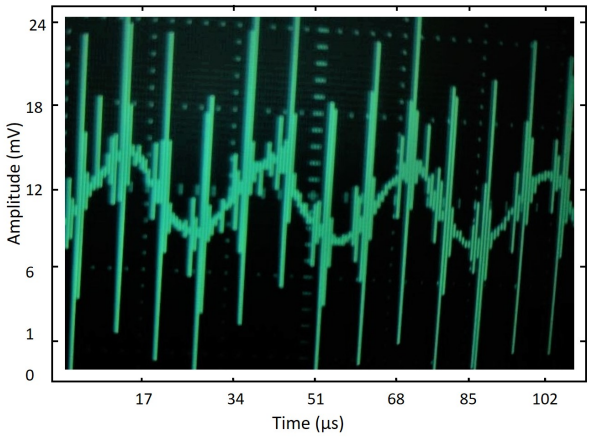

(a) Red LED channel

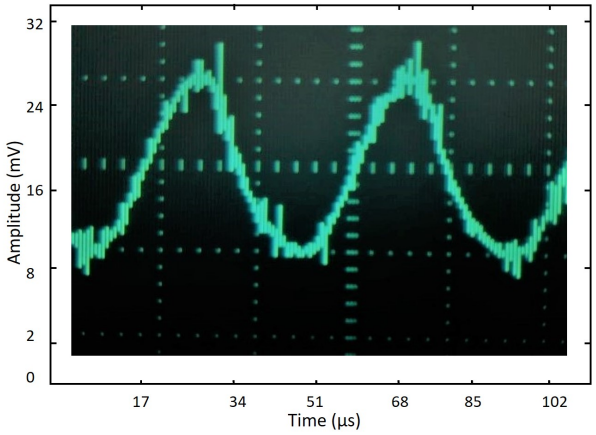

(b) Green LED channel

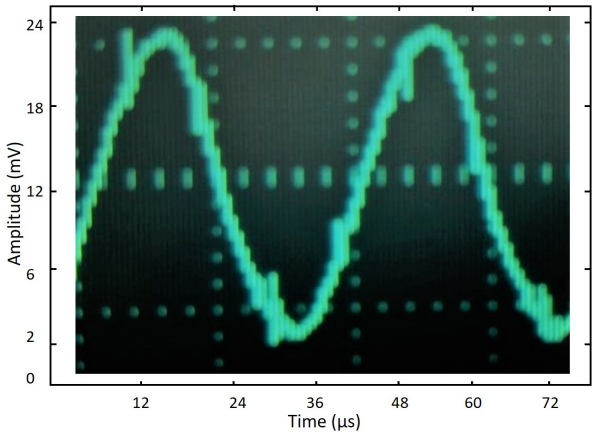

(c) Blue LED channel

Fig. 8. Solar panel voltage response for maximum bandwidth and $R_L = 1\ k\Omega$.

The maximum data rate achieved experimentally with OOK modulation is presented in Fig. 9. We evaluated the bit-error-rate (BER) performance of the proposed solar panel receiver-based VLC system with each RGB channel and parallel

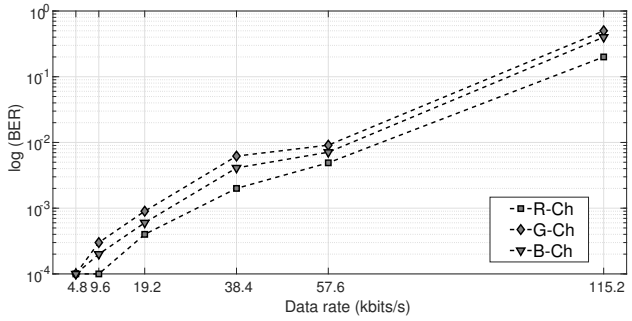

Fig. 9. Measured BER performance with each RGB channel of the proposed solar panel receiver-based VLC system with a parallel resistance $R_L = 1\ k\Omega$ at different data rates.

resistance $R_L = 1\ k\Omega$ at different data rates. The distance between the transmitter and the receiver was $105\ cm$. From Fig. 9, we can observe that, at a data rate of $4800\ bits/s$, a BER of 1.1×10^{-4} can be achieved for all the channels. When the data rate is increased to $38400\ bits/s$, BER of 2×10^{-3}, 4×10^{-3}, and 6.2×10^{-3}, can be obtained with the red, green, and blue channels, respectively. We can also see that the maximum data rate is limited by the low bandwidth of the solar panel ($28.3\ kHz$ with the red channel and $R_L = 1\ k\Omega$, see Fig. 7a). Nevertheless, we consider that having a solar panel as a VLC receiver with a small $R_L (< 1\ k\Omega)$ improves the frequency response and data rate of the VLC system, however, this affects the signal-to-noise ratio (see Fig. 8a).

V. Conclusions

This paper presents an evaluation of the bandwidth of a solar panel-based receiver for RGB LED channels in a visible light communication system. We proposed a method to identify the optical-to-electrical response and bandwidth of a solar panel under different wavelengths. Adopting this method, we determined that the bandwidth of the solar panel-based receiver is higher when using parallel load resistors of low value and a red-light source as the transmitter. The maximum bandwidth of the solar panel was $28.3\ kHz$, $23\ kHz$, and $27\ kHz$ for the red, green, and blue LEDs, respectively. With this configuration method, the solar panel produced low voltage levels, and, as a consequence, the resulting signal-to-noise ratio became smaller. It could have an impact on the speed of the VLC system, but we consider the latter to be functional because the target applications are for low-data-rate scenarios; therefore, the bit rate is not critical. Our experimental results show that the solar panel can achieve a transmission speed of $57600\ bits/s$ and a BER of 5×10^{-3} with the red channel at a free space transmission distance of $105\ cm$. Thus, we conclude that RGB LEDs can increase the energy generation and communication capacity of solar panels.

The proposed structure has the potential to enable VLC applications with low-cost and low-rate architectures such as sensor networks, indoor visible light positioning systems, and music streaming. As solar panels become more affordable and easy to integrate with wearable devices, their integration into VLC systems will eventually allow for more energy-efficient visible light access control systems. Future work could address three topics related to the duality of the use of solar panels: (1) energy harvesting using RGB light sources; (2) bandwidth improvement of solar panel receivers for VLC systems; and (3) integration of wavelength division multiplexing (WDM) with RGB LED to improve performance and reduce the negative effect of noise.

References

[1] A. Chizari, M. V. Jamali, S. Abdollahramezani, J. A. Salehi, and A. Dargahi, "Visible light for communication, indoor positioning, and dimmable illumination: A system design based on overlapping pulse position modulation," *Optik*, vol. 151, no. 2017, pp. 110–122, 2017.

[2] M. Katz and D. O'Brien, "Exploiting novel concepts for visible light communications: from light-based iot to living surfaces," *Optik*, vol. 195, no. August, p. 163176, 2019.

[3] L. E. M. Matheus, A. B. Vieira, L. F. Vieira, M. A. Vieira, and O. Gnawali, "Visible Light Communication: Concepts, Applications and Challenges," *IEEE Communications Surveys and Tutorials*, vol. 21, no. 4, pp. 3204–3237, 2019.

[4] Y. Zhuang, L. Hua, L. Qi, J. Yang, P. Cao, Y. Cao, Y. Wu, J. Thompson, and H. Haas, "A survey of positioning systems using visible led lights," *IEEE Communications Surveys & Tutorials*, vol. 20, no. 3, pp. 1963–1988, 2018.

[5] "Ieee standard for local and metropolitan area networks - part 15.7: Short-range optical wireless communications," *IEEE Std 802.15.7-2018 (Revision of IEEE Std 802.15.7-2011)*, pp. 0–407, 2019.

[6] J. Luo, L. Fan, and H. Li, "Indoor positioning systems based on visible light communication: State of the art," *IEEE Communications Surveys & Tutorials*, vol. 19, no. 4, pp. 2871–2893, 2017.

[7] R. Ji, S. Wang, Q. Liu, and W. Lu, "High-Speed Visible Light Communications: Enabling Technologies and State of the Art," *Applied Sciences*, vol. 8, p. 589, apr 2018.

[8] O. Saied, Z. Ghassemlooy, S. Rajbhandari, and A. Burton, "Optical single carrier-interleaved frequency division multiplexing for visible light communication systems," *Optik*, vol. 194, no. May, p. 162910, 2019.

[9] X. Song, S. Xing, M. Wang, and Q. Wang, "Effect of driving current on phosphorescent white LED and a second-order hardware pre-equalization strategy for VLC in military vehicle," *Optik*, vol. 185, no. October 2018, pp. 1096–1103, 2019.

[10] R. A. Martínez, F. E. López, and A. F. Betancur, "RGB Sensor Frequency Response for a Visible Light Communication System," *IEEE Latin America Transactions*, vol. 14, no. 12, pp. 4688–4692, 2016.

[11] R. A. Martínez, F. E. López, A. F. Betancur, and J. M. Luna, "Design and Implementation of a Multi-Colour Visible Light Communication System Based on a Light-to-Frequency Receiver," *Photonics*, vol. 6, no. 42, pp. 1–17, 2019.

[12] F. Seguel, N. Krommenacker, P. Charpentier, and I. Soto, "A novel range free visible light positioning algorithm

for imaging receivers," *Optik*, vol. 195, no. June 2019, p. 163028, 2019.

[13] P. Chavez-Burbano, V. Guerra, J. Rabadan, and R. Perez-Jimenez, "Optical Camera Communication system for three-dimensional indoor localization," *Optik*, vol. 192, p. 162870, sep 2019.

[14] Z. Wang, D. Tsonev, S. Videv, and H. Haas, "On the Design of a Solar-Panel Receiver for Optical Wireless Communications with Simultaneous Energy Harvesting," *IEEE Journal on Selected Areas in Communications*, vol. 33, no. 8, pp. 1612–1623, 2015.

[15] P. A. Loureiro, F. P. Guiomar, and P. P. Monteiro, "Visible Light Communications: A Survey on Recent High-Capacity Demonstrations and Digital Modulation Techniques," *Photonics*, vol. 10, no. 9, 2023.

[16] B. Genovés Guzmán and V. P. Gil Jiménez, "Dco-ofdm signals with derated power for visible light communications using an optimized adaptive network-based fuzzy inference system," *IEEE Transactions on Communications*, vol. 65, no. 10, pp. 4371–4381, 2017.

[17] H.-W. Chen, S.-S. Wen, X.-L. Wang, M.-Z. Liang, M.-Y. Li, Q.-C. Li, and Y. Liu, "Color-shift keying for optical camera communication using a rolling shutter mode," *IEEE Photonics Journal*, vol. 11, no. 2, pp. 1–8, 2019.

[18] J. M. Luna, V. Guerra, J. Rufo, R. Perez, C. Suarez, and J. Rabadan, "Low-complexity colour-shift keying-based visible light communications system," *IET Optoelectronics*, vol. 9, no. 5, pp. 191–198, 2015.

[19] Z. Babar, C. Zhu, H. V. Nguyen, P. Botsinis, D. Alanis, D. Chandra, S. X. Ng, and L. Hanzo, "Reduced-Complexity Iterative Receiver for Improving the IEEE 802.15.7 Convolutional-Coded Color Shift Keying Mode," *IEEE Communications Letters*, vol. 21, no. 9, pp. 2005–2008, 2017.

[20] F. M. Wu, C. T. Lin, C. C. Wei, C. W. Chen, Z. Y. Chen, H. T. Huang, and S. Chi, "Performance comparison of OFDM signal and CAP signal over high capacity RGB-LED-based WDM visible light communication," *IEEE Photonics Journal*, vol. 5, no. 4, 2013.

[21] W. D. Leon and X. Fan, "Solar Cell Photo-Luminescence Modulation for Optical Frequency Identification Devices," *IEEE Transactions on Circuits and Systems I: Regular Papers*, vol. 66, no. 5, pp. 1981–1992, 2018.

[22] Y. Liu, H.-Y. Chen, K. Liang, C.-W. Hsu, C.-W. Chow, and C.-H. Yeh, "Visible Light Communication Using Receivers of Camera Image Sensor and Solar Cell," *IEEE Photonics Journal*, vol. 8, no. 1, pp. 1–7, 2016.

[23] H. Y. Wang, J. T. Wu, C. W. Chow, Y. Liu, C. H. Yeh, X. L. Liao, K. H. Lin, W. L. Wu, and Y. Y. Chen, "Using pre-distorted PAM-4 signal and parallel resistance circuit to enhance the passive solar cell based visible light communication," *Optics Communications*, vol. 407, no. April 2017, pp. 245–249, 2018.

[24] J. T. Wu, C. W. Chow, Y. Liu, C. W. Hsu, and C. H. Yeh, "Performance enhancement technique of visible light communications using passive photovoltaic cell," *Optics Communications*, vol. 392, no. November 2016, pp. 119–122, 2017.

[25] Z. Tong, X. Yang, Y. Gao, H. Zhang, Y. Zhang, X. Wang, and J. Xu, "A long-distance underwater wireless optical link enabled by a solar array with a baseline compensator," *IEEE Photonics Journal*, vol. 15, no. 3, pp. 1–8, 2023.

[26] X. Ke, Y. Xu, H. Qin, and J. Liang, "Research on Resource Allocation Strategy of Indoor Visible Light Communication and Radio Frequency Systems Integrating Orthogonal Frequency-Division Multiple Access Technology," *Photonics*, vol. 10, no. 9, 2023.

[27] R. A. Martínez, F. E. López, A. F. Betancur, and J. M. Luna, "Characterization of Light-To-Frequency Converter for Visible Light Communication Systems," *Electronics*, pp. 1–11, 2018.

[28] A. D. Dhass, N. Beemkumar, S. Harikrishnan, and H. M. Ali, "A Review on Factors Influencing the Mismatch Losses in Solar Photovoltaic System," *International Journal of Photoenergy*, vol. 2022, pp. 1–27, 2022.

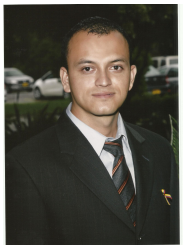

Roger Alexander Martínez Ciro received the bachelor's degree in telecommunication engineering, the master´s degree in automation and industrial control and the Ph.D. degree in Engineering from the Metropolitan Institute of Technology of Medellín, Colombia in 2015, 2018 and 2023 respectively. He is currently a research professor at engineering faculty of the Metropolitan Institute of Technology, Colombia since 2018. His research interests includes Optical Wireless Communication, Indoor Positioning and Visible Light Communication.

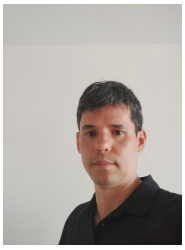

Francisco Eugenio López Giraldo received the B.Sc. degree in Physics on Quantum Optics in 2003, the M.Sc. degree in Physics on Many-Body Interactions in Semiconductors in 2007 and Ph.D in Physics on Semiconductor Nanostructures in 2009 from the Antioquia University of Colombia. During his Ph.D. studies in Semiconductor Nanostructures at the Antioquia University (2006 - 2009), he study of electronic and optic properties of semiconductor nanostructures, specifically the Landè g Factor. In 2008, he worked in UNICAMP on Optical Properties of Semiconductor Heterostructures. He is currently a research professor at engineering faculty of the Metropolitan Institute of Technology, Colombia since 2009. His research interests includes Antennas, Wireless Communication and Visible Light Communication.

Jose Martin Luna-Rivera received the B.S. and M.Eng. degrees in electronics engineering from the Autonomous University of San Luis Potosi, Mexico, in 1997 and 1998, respectively, and the Ph.D. degree in electrical engineering from The University of Edinburgh, U.K., in 2003. He is currently a full-time Professor with the Faculty of Sciences, Autonomous University of San Luis Potosi. His research interests include a broad spectrum of areas within signal processing for wireless communication systems. He has pioneered techniques and algorithms for array signal detection, efficient modulation schemes, transmit/receive diversity schemes, channel modeling, signal precoding, interference cancellation, and power control techniques. Moreover, with the rapid advancements in the field, he has also delved into integrating machine learning methodologies to enhance wireless communication systems' adaptability and efficiency. His research has found applications in domains such as visible light communications, vehicular communications, the Internet of Things, and mobile communications. He has authored and contributed to over 100 journal articles and refereed conference publications.

Juan David Rojas Usuga received the bachelor's degree in electronic engineering from the Metropolitan Institute of Technology, Colombia in the 2021. He is currently a master's degree in electronic automation and industrial control from the Metropolitan Institute of Technology. His research interests include Visible Light Communications, Direction-of-arrival, machine learning.

Juan David Navarro Restrepo his bachelor's degree in Telecommunications Engineering in the Metropolitan Institute of Technology (ITM) 2020. Early in his career, he has shown a strong commitment to the dissemination of scientific knowledge, participating in international lectures and publishing in journals with related topics of Visible Light Communication. Since 2016, Juan evidenced some interests in the phenomenon of light which led him to join research groups, where he quickly developed a passion to find out answers difficult questions and knowledge to move forward. He made important contributions around the characterization of LEDs and the study of photodetectors for indoor systems considered for low data transfer applications. Currently, Juan David is pursuing a Master's degree in Automation and Industrial Control at ITM. He is looking forward to investigate innovative telecommunications solutions with social impact.